JVI Journals.ASM.org

Conservation of the STING-Mediated Cytosolic DNA Sensing Pathway in Zebrafish

Rui Ge,[a] Yi Zhou,[a] Rui Peng,[a] Rui Wang,[a] Mi Li,[a] Yunbin Zhang,[a] Chunfu Zheng,[b] Chen Wang[a]

State Key Laboratory of Cell Biology, Institute of Biochemistry and Cell Biology, Shanghai Institutes for Biological Sciences, Chinese Academy of Sciences, Shanghai, China[a]; Institutes of Biology and Medical Sciences, Soochow University, Suzhou, China[b]

ABSTRACT

Zebrafish (*Danio rerio*) is a unique potential model animal for dissecting innate immune signaling. Here we demonstrate that herpes simplex virus 1 (HSV-1) could infect zebrafish at its different developmental stages and trigger the expression of type I interferons (IFNs) as well as interferon-stimulated genes (ISGs) in zebrafish larvae. Silencing of zSTING, but not zMAVS, markedly attenuates the DNA virus-induced antiviral responses. Notably, a conserved serine residue (S373) is essential for the action of zSTING. Unexpectedly, zebrafish cyclic GMP-AMP synthase (cGAS) is dispensable for the STING signaling, whereas zDHX9 and zDDX41 are potential sensors for HSV-1 infection *in vivo*. Taken together, this proof-of-concept study establishes the zebrafish larva as a feasible model for investigating the cytosolic DNA sensing mechanism, shedding light on the conservation of the STING antiviral signaling pathway.

IMPORTANCE

The zebrafish larva provides technical advantages for understanding host-pathogen interactions. In this study, we established the zebrafish larva as a useful model for studying HSV-1 infection. HSV-1 infection triggers strong type I interferon production, which depends on STING expression. In addition, STING-mediated antiviral signaling is conserved in zebrafish. Interestingly, zDHX9 and zDDX41 are indispensable for detecting HSV-1, while cGAS is dispensable. This proof-of-concept study indicates that the zebrafish represents an amenable model for the investigation of cytosolic DNA sensing mechanisms.

The zebrafish (*Danio rerio*) early larva has been successfully employed in elucidating the molecular mechanisms of embryogenesis (1). The last decade has witnessed its accelerated expansion to address the evolution and the development of the immune system (2, 3). The zebrafish displays several favorable advantages as an effective model organism, which complements the application spectrum of mouse models. For examples, the zebrafish is much more amenable to forward and/or reverse genetic screens. Additionally, it is available for *in vivo* real-time visualization, due to the optical transparency of zebrafish larvae (4, 5). Some human disease models were established in zebrafish (6) and are instrumental for identification and characterization of the evolutionarily conserved genes that are important in human pathology (5, 7–9). Notably, a cutting-edge area of study is to establish effective virus infection models and employ them for dissecting the innate antiviral signaling in zebrafish (10–15).

In mammals, cytosolic RNA and DNA viruses are sensed/recognized by their corresponding receptors, which ultimately activate the IRF3- and/or NF-κB-responsive genes, including type I interferons (IFNs) and proinflammatory cytokines (16, 17). RIG-I and MDA5 specifically recognize the RNA viruses and trigger the activation of TBK1 and IRF3 via the mitochondrial adaptor MAVS (18, 19). Cytosolic DNA viruses are sensed by a set of different receptors (cyclic GMP-AMP synthase [cGAS], IFI16, DHX9, and DDX41) (20–24). Signaling pathways initiated by these receptors apparently converge on the stimulator of interferon genes (STING) (also known as MITA, ERIS, or MPYS), a transmembrane protein in the endoplasmic reticulum (ER) (25–28). It remains to be elucidated how STING activates TBK1 and IRF3. The RIG-I/MAVS signaling is well conserved in zebrafish (29, 30). However, little is known about the STING signaling of zebrafish (31).

There are four virus-induced IFN genes in zebrafish (known as IFN-φ), which structurally belong to type I IFNs (32, 33). Like those in mammals, zebrafish IFNs impair viral replication via induction of a large number of interferon-stimulated genes (ISGs) (34). The orthologs of mammalian ISGs have been identified in zebrafish (*isg15*, *viperin/vig1*, and *Mx*), and they apparently perform similar functions. For example, zf-isg15 triggers a strong antiviral activity against RNA and DNA viruses in fish cells (35).

Herpes simplex virus 1 (HSV-1) belongs to the alphaherpesviruses subfamily. HSV-1 infects permissive host cells (epithelial cells) to initiate lytic infection and establishes latent infection specifically in neurons (36). HSV-1 infection has been extensively employed to elucidate STING signaling in mice (25, 37). Some preliminary studies suggested that HSV-1 could potentially infect zebrafish and persist in adult zebrafish brain (13, 38). It remains unknown whether HSV-1 infection could be adapted to explore cytosolic DNA signaling in zebrafish. In this study, we successfully established the HSV-1 infection model in zebrafish larvae. Further exploration revealed the conservation of STING signaling in zebrafish. Unexpectedly, zebrafish cGAS is dispensable for the

Received 22 April 2015 Accepted 8 May 2015
Accepted manuscript posted online 13 May 2015
Citation Ge R, Zhou Y, Peng R, Wang R, Li M, Zhang Y, Zheng C, Wang C. 2015. Conservation of the STING-mediated cytosolic DNA sensing pathway in zebrafish. J Virol 89:7696–7706. doi:10.1128/JVI.01049-15.
Editor: L. Hutt-Fletcher
Address correspondence to Chen Wang, cwang01@sibcb.ac.cn.

doi:10.1128/JVI.01049-15

STING signaling, whereas zDHX9 and zDDX41 are potential sensors for HSV-1 infection *in vivo*. This proof-of-concept study establishes the zebrafish larva as a feasible model for investigating the cytosolic DNA sensing mechanism, paving the way for future large-scale screening.

MATERIALS AND METHODS

Zebrafish maintenance and embryo production. Zebrafish maintenance, breeding, and staging were performed as described previously (1). Zebrafish embryos were acquired by natural spawning and kept at 28.5°C in incubator. After inoculation, the larvae were transferred to a gnotobiotic water system for further experiments.

Manipulation of viruses. Wild-type HSV-1 and HSV-1-green fluorescent protein (GFP) were propagated and titers determined by plaque assays on Vero cells.

Riboprobe synthesis and WISH. Antisense riboprobes for HSV-1 ICP0 were synthesized using a digoxigenin (DIG) RNA labeling kit (Roche) according to the manufacturer's instructions. To construct the ICP0 probe, the ICP0 open reading frame (ORF) (from bp 68 to 1100) was amplified from the HSV-1 genome using primers 5′-ATGTCTGGGTGT TTCCCTGCGACCGAGACCTGC and 3′-AAGTCGCTGATCACTATG GGGTCTCTGTTGTTT, and then the product was cloned into the BAmHI and XhoI sites of the pcDNA3.0 vector. Whole-mount *in situ* hybridization (WISH) was carried out as described previously, and staining was performed with an alkaline phosphatase substrate kit (Promega).

MOs, mRNA synthesis, and microinjection. All morpholinos (MOs) were ordered from Gene Tools and dissolved with nuclease-free H_2O to 1 mM as stock solutions. The MOs were control (5′-GCGATCATAGCTG CAAAAGACCAAA-3′), zSTING (5′-GAGCGTCTTCTCCCATCACAG ACAT-3′), zpcGAS (5′-CTGGTCTCCTGTGGCTGCTCATGAT-3′), zDDX41 (5′-GCTCGGTTTTCCGTTTCCATAATGC-3′), zDHX9 (5′-G GAAGTTCTTAATGTCCGCCATTGC-3′), and zMAVS (5′-GCAAAAC GACCCATATACGGCCTAA-3′), which all target the start codon regions of the zebrafish sequence. The standard control morpholino from Gene Tools was used as a control for nonspecific effects.

For mRNA synthesis, human, mouse, and zebrafish STING full-length cDNA sequences were cloned into the pcDNA3.0 vector with BamHI and XhoI. The zebrafish STING S373A mutation was cloned using primers 5′-GACGAGCCCACCCTCATGTTCGCCCGACCT and 3′-GGATCTT AGGGATTGAGGTCGGGCGAACAT. Capped mRNA was synthesized using the mMESSAGE kit (Ambion) and purified with Mini Quick Spin RNA columns (Roche). MOs and mRNAs were injected into 1-cell-stage zebrafish embryos at the yolk/blastomere boundary. For HSV-1 inoculation, HSV-1 was injected into the hindbrain ventricle (HBV) or caudal vein (CV) in zebrafish larvae at 72 h postfertilization (hpf).

Real-time quantitative PCR. Total RNAs were extracted from 15 zebrafish larvae using TRIzol reagent (Invitrogen). RNA was reverse transcribed using oligo(dT) and Moloney murine leukemia virus (M-MLV) reverse transcriptase (Promega), and 2× PCR mix (Roche) was used for the real-time quantitative PCR analysis. All values were normalized to the level of GAPDH (glyceraldehyde-3-phosphate dehydrogenase) mRNA. The forward and reverse primers used for zebrafish were as follows: GAPDH, 5′-CTTTGGTATTGAGGAGGCT-3′ (sense) and 5′-GGATGA TGTTCTGGTGGG-3′ (antisense); IFN-φ1, 5′-TGAGAACTCAAATGT GGACCT-3′ (sense) and 5′-GTCCTCCACCTTTGACTTGT-3′ (antisense); ISG15, 5′-ATGCAGCTGACTGTAAAACT-3′ (sense) and 5′-TT ATCCTCCTCGTAGACGGA-3′ (antisense); viperin, 5′-GCTGAAAGAA GCAGGAATGG-3′ (sense) and 5′-AAACACTGGAAGACCTTCCAA-3′ (antisense); HSV polymerase, 5′-GCTCGAGTGCGAAAAAACGTTC-3′ (sense) and 5′-TGCGGTTGATAAACGCGCAGT-3′ (antisense); and HSV ICP22, 5′-GTGCAAGCTTCCTTGTTTGG-3′ (sense) and 5′-GGT GGCATCGGAGATTTCAT-3′ (antisense).

HSV-1 genomic DNA isolation. To extract HSV-1 genomic DNA, we used standard phenol-chloroform extraction methods. Briefly, the 15 zebrafish larvae infected with HSV-1 were resuspended in 200 μl lysis buffer (10 mM EDTA,10 mM Tris-HCl [pH 8.0], 1% SDS) containing proteinase K (200 μg/ml). The samples were shaken overnight at 55°C and extracted with phenol-chloroform-isoamyl alcohol (25:24:1) and with 1 ml of chloroform-isoamyl alcohol (24:1). The aqueous phase was precipitated with ice-cold ethanol (100%). The DNA pellet was then washed with ethanol (70%), air dried for 10 min, and resuspended in 50 μl double-distilled water (ddH_2O), and the concentration was measured.

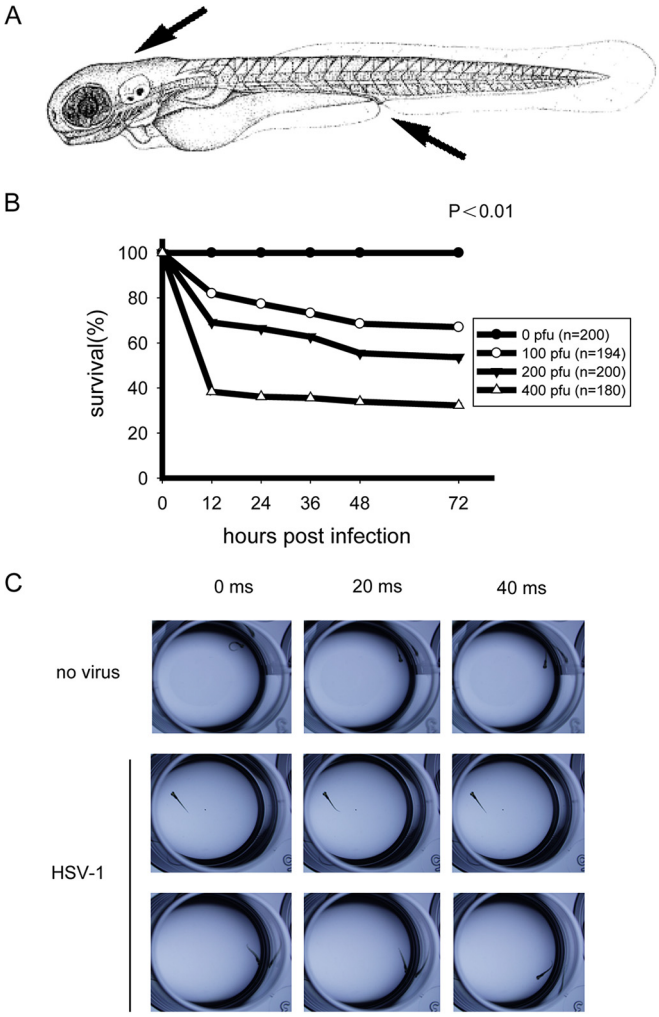

FIG 1 HSV-1 can successfully infect zebrafish larvae. (A) Diagram of the inoculation sites in larvae at 72 h postfertilization (hpf) (arrows), i.e., hindbrain ventricle and caudal vein. (B) Survival rates of wild-type infected zebrafish larvae. AB strain zebrafish larvae were injected at 72 hpf with the indicated dose of wild type HSV-1 per larva, and the survival rates were monitored for 72 h postinfection (hpi). (C) Uninfected (no virus) or wild-type HSV-1-infected zebrafish larvae (48 hpi) were tested for behavioral changes. The larvae were placed in 12-well plates, and locomotion activities were recorded with a high-speed camera.

GFP reporter assay. To verify the efficacies and specificities of the zSTING, zpcGAS, zDDX41, zDHX9, and zMAVS morpholinos, pCS2-GFP reporter plasmids which harbor each morpholino target sequence in the 5′ untranslated region of the GFP transcript were created. Capped mRNA was synthesized by each of these plasmids, and then the capped mRNA (150 ng/ml) was injected into 1-cell zebrafish embryos with control MO or the specific targeting morpholino (0.3 mM) to mark successfully injected embryos. At 12 hpf, embryos were assayed for GFP fluorescence. The forward and reverse primers used were as follows: zSTING, 5′-ATCAAGCTTATGTCTGTGATGGGAGAAGA-3′ (sense) and 5′-AT CGGATCCAAAGCGATAATTCCAGCTC-3′ (antisense); zpcGAS, 5′-A

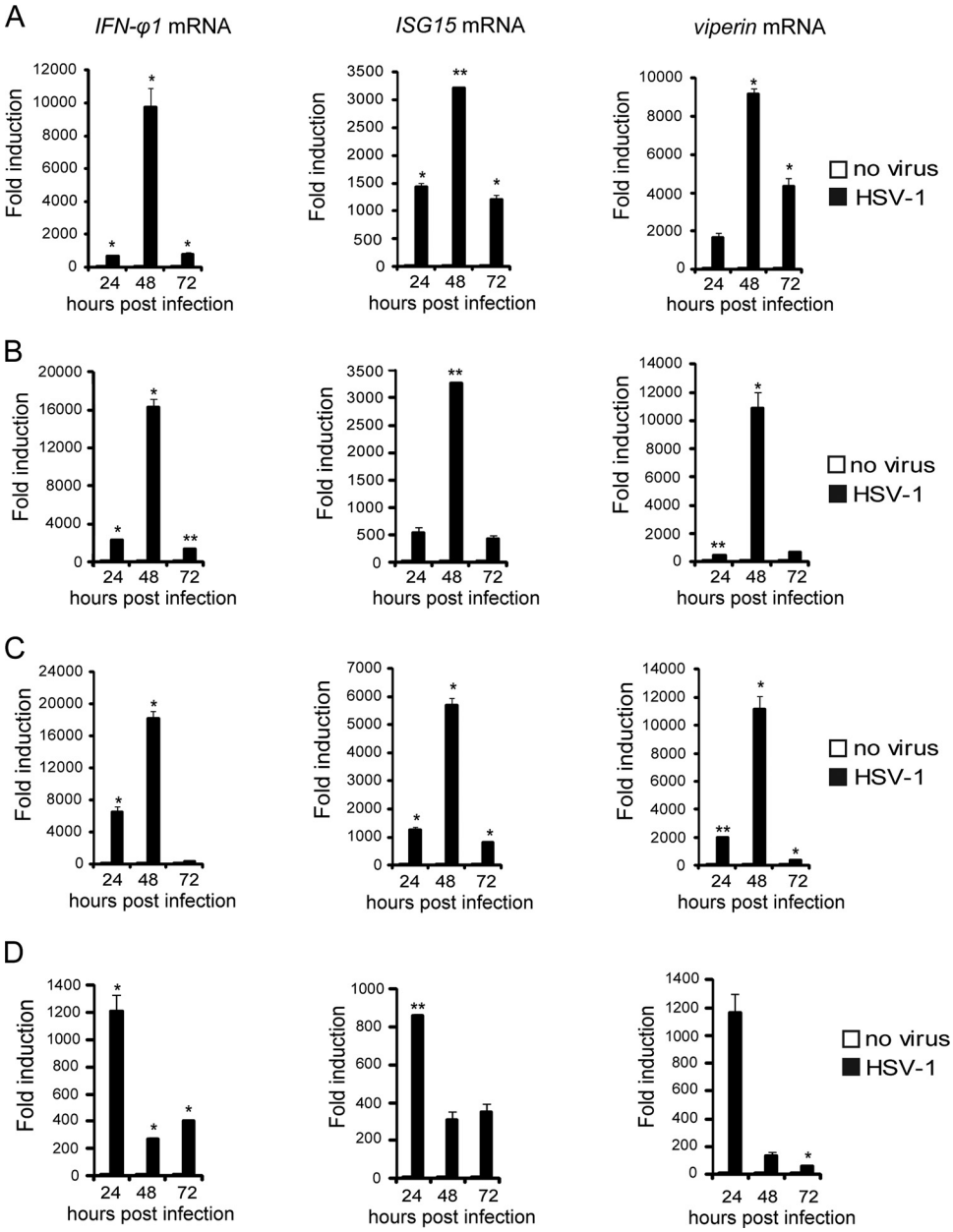

FIG 2 HSV-1 can infect zebrafish larvae at different development stages. Zebrafish larvae at 48 hpf (A), 60 hpf (B), 72 hpf (C), and 96 hpf (D) were inoculated with 0 PFU (no virus) or 200 PFU wild-type HSV-1. Induction of IFN-φ1, ISG15, and viperin mRNAs was measured via real-time quantitative PCR at the indicated time points. Assays were performed on RNA extracted from entire larvae and measured values normalized to the control set. Data shown are mean ± SEM from at least three independent experiments, *, $P < 0.05$; **, $P < 0.01$ (versus the corresponding control).

TCAAGCTTATGAGCAGCCACAGGAGACC-3′ (sense) and 5′-ATCGGATCCTGAAGTTTGGCTTCACTTTC-3′ (antisense); zDDX41, 5′-ATCAAGCTTATGGAAACGGAAAACCGAGC-3′ (sense) and 5′-ATCGGATCCCCTTTACCCCGCAGACGCA-3′ (antisense); zDHX9, 5′-ATCAAGCTTATGGCGGACATTAAGAACTT-3′ (sense) and 5′-ATCGGATCCTTTCCCATACCGATGTAAC-3′ (antisense); and zMAVS, 5′-ATCAAGCTTATGGGTCGTTTTGCAACAGA-3′ (sense) and 5′-ATCGGATCCCTGCGCAGATTGTCCAGAA-3′ (antisense).

***In vivo* confocal imaging and data analysis.** Zebrafish larvae were fixed in 1.2% agarose and scanned with a Leica laser scanning confocal microscope. The images were generated by three-dimensional (3D) projections with Leica LAS AF Lite software. The density of GFP was calculated with Image J analysis software (NIH).

Locomotion test and capture. Infected zebrafish larvae (48 hpi) were put into 12-well plates and recorded under a microscope (MZ16F; Leica) with an attached high-speed camera (Redlake MotionScope M3, 1,000 fps). Each larva was tested 8 to 10 times.

Statistical analysis. Quantitative data are expressed as mean ± standard error of the mean (SEM). Statistical significance was determined by two-way analysis of variance (ANOVA). A P value of less than 0.05 was considered statistically significant.

RESULTS

HSV-1 infects zebrafish larvae successfully. Zebrafish larvae hatch from chorion and develop to maturity at 72 h postfertiliza-

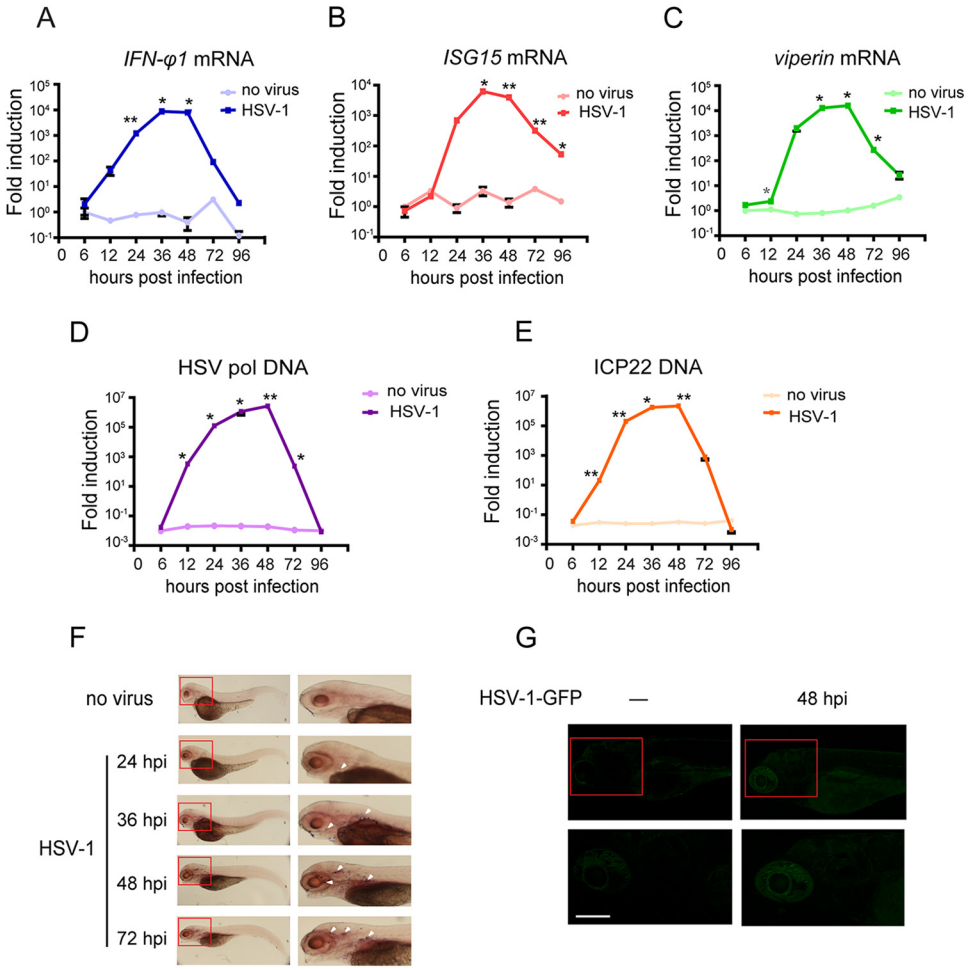

FIG 3 Host antiviral response to HSV-1 infection in zebrafish larvae. (A to C). Zebrafish larvae were stimulated with 0 PFU or 200 PFU wild-type HSV-1 and monitored for the indicated times. Induction of IFN-φ1, ISG15, and viperin mRNAs was measured by real-time quantitative PCR. Assays were performed on RNA extracted from entire larvae and measured values normalized to the control set. Data shown are mean ± SEM from at least three independent experiments. *, $P < 0.05$; **, $P < 0.01$ (versus the corresponding control). (D and E) HSV-1 replicated in zebrafish larvae, and its replication status was demonstrated by HSV-1 genomic DNA levels. Zebrafish larvae were stimulated with 0 PFU or 200 PFU wild-type HSV-1 and harvested at the indicated time points. Genomic DNA was extracted for real-time quantitative PCR analysis of HSV-1 polymerase (pol) and ICP22 genomic DNA levels. (F) Whole-mount *in situ* hybridization of uninfected or intravenously HSV-1-challenged 72-hpf zebrafish larvae. Representative images of propylthiouracil (PTU)-treated larvae inoculated and fixed at the indicated times with riboprobe against HSV-1 ICP0 (36 hpi for uninfected control) are shown. The right panels represent the areas of the red boxes in the left panels. Arrowhead denote the locations of HSV-1 distribution. (G) Confocal imaging of intravenously PBS-treated or HSV-1-GFP-infected zebrafish larvae at 48 hpi. The lower panels represent the confocal image areas of the red boxes in the corresponding upper panels. HSV-1-GFP accumulated mainly in larva brain. Viral particles are markedly observed in infected larvae compared to control larvae. Scale bars, 50 μm.

tion (hpf). First, we tested whether the zebrafish was susceptible to HSV-1 infection at 28°C. Wild-type HSV-1 (0 to 400 PFU) were injected into the hindbrain ventricles (HBV) or caudal veins (CV) of the larvae (Fig. 1A). We observed that mortality of infected larvae occurred in a dose-dependent manner (Fig. 1B). The dose of 200 PFU was applied for all subsequent experiments. The infected larvae were dissected at the indicated time points, and behavioral disorders were examined via swimming patterns and locomotor activity. Notably, HSV-1-infected larvae were markedly crippled or lost rapid change in locomotor activity (Fig. 1C). Collectively, these data indicate that HSV-1 could infect zebrafish larvae successfully.

HSV-1 induces robust antiviral responses in zebrafish. We went on to explore whether HSV-1 could infect the zebrafish larvae at different developmental stages. The mRNA expression levels of antiviral genes were measured at 24 hours postinfection (hpi), 48 hpi, and 72 hpi for zebrafish larvae at 48 hpf (Fig. 2A), 60 hpf (Fig. 2B), 72 hpf (Fig. 2C), and 96 hpf (Fig. 2D). It was observed that HSV-1 could induce robust host responses in zebrafish larvae at different developmental stages. However, the time windows of the responses were slightly different among the larvae (Fig. 2A to D). For experimental convenience, HSV-1 infection of the zebrafish larvae was always at 72 hpf for all the experiments, except where explicitly indicated otherwise.

To further characterize this infection model, we monitored the time course of the mRNA expression levels of the IFN-φ1 gene and the IFN-responsive genes (ISG15 and viperin) in 72-hpf larvae via quantitative reverse transcription-PCR (RT-PCR). It was observed that IFN-φ1 was induced as early as 12 hpi, and this induc-

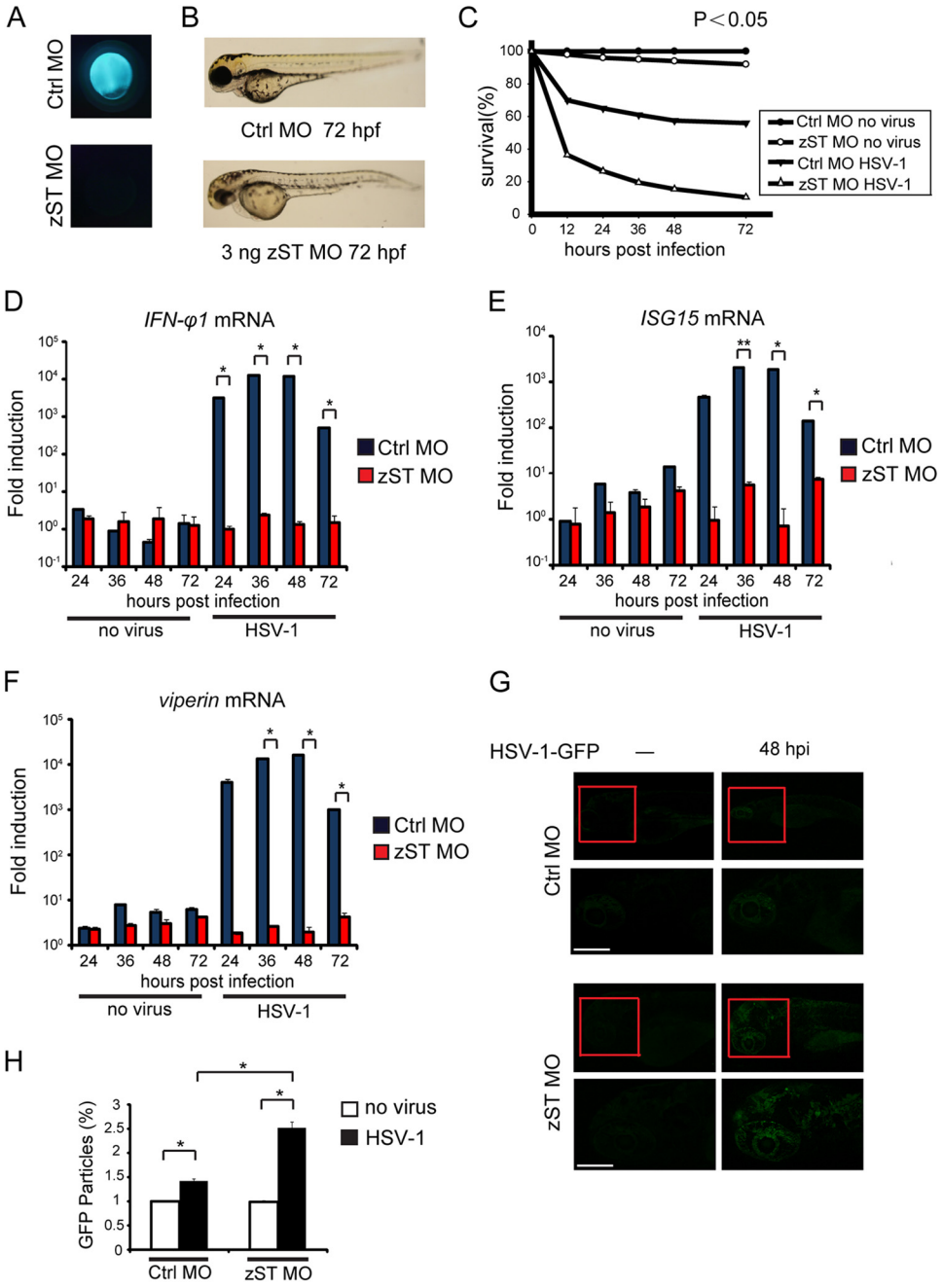

FIG 4 STING signaling is conserved in zebrafish larvae. (A) Morpholino-based zSTING gene knockdown is efficient in zebrafish embryos. (B) Phenotypic analyses of zebrafish larvae at 72 hpf. Embryos were injected with 3 ng control morpholino (Ctrl.MO) or 3 ng zebrafish STING MO (zST MO). The morphological defects of zST morphant larva were analyzed at 72 hpf. (C) Survival rates of HSV-1-infected zebrafish morphants. Two hundred AB zebrafish embryos were injected with control or STING morpholino at the 1-cell stage and raised to 72 hpf, and then every larva was inoculated with 0 PFU or 200 PFU wild-type HSV-1 and survival rates were monitored for 72 h postinfection (hpi). (D to F) Real-time quantitative PCR (RT-PCR) verification of antiviral genes induction in HSV-1 infection. Control morphants and zST morphants were stimulated with 200 PFU wild-type HSV-1 for the indicated time periods. Induction of IFN-φ1 (D), ISG15 (E), and viperin (F) mRNAs was measured by real-time quantitative PCR. (G) Confocal imaging of uninfected or HSV-1-GFP-inoculated morphants at 48 hpi. Embryos were injected with 3 ng control morpholino or STING morpholino and raised to 72 hpf for HSV-1-GFP inoculation. At 48 h postinfection (hpi), larvae were embedded in 1.2% agarose and visualized by Leica laser scanning confocal microscopy. The lower panels represent the confocal image areas of the red boxes in the upper panels. All the larvae are shown in lateral views with rostral side left and dorsal side up. Scale bars, 50 μm. (H) Quantification of GFP-positive particles in infected morphant larvae. The density of GFP was calculated with Image J (NIH). Data shown are mean ± SEM from at least three independent experiments. *, $P < 0.05$.

tion peaked at approximately 36 hpi and then steadily dropped until 96 hpi (Fig. 3A). The inductions of the ISG15 and viperin genes (also known as *vig1* or *rsad2*) were similar to that for IFN-φ1 (Fig. 3B and C). The HSV-1 genomic DNA levels in the infected zebrafish larva were analyzed by the levels of HSV-1 polymerase and ICP22 DNAs (Fig. 3D and E).

The localization of HSV-1 in zebrafish larvae was revealed by whole-mount *in situ* hybridization (WISH), using the DIG-la-

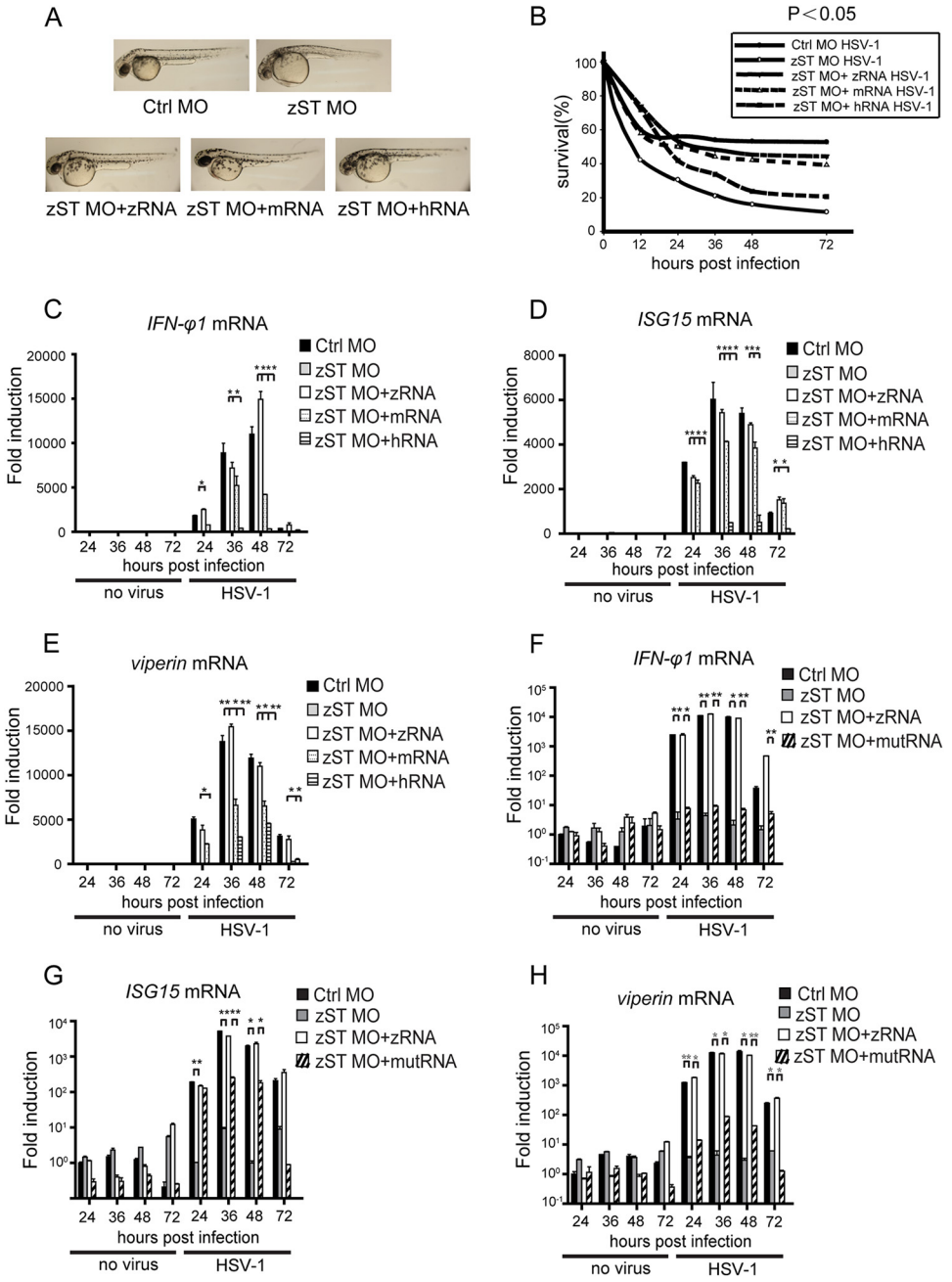

FIG 5 STING mRNA can rescue host antiviral activity. (A) Phenotypic analyses of rescued larvae at 72 hpf. Embryos were injected with 3 ng control morpholino (Ctrl MO), 3 ng zSTING MO, 3 ng zSTING MO plus 150 pg zSTING-mRNA, 3 ng zSTING MO plus 150 pg mSTING-mRNA, and 3 ng zSTING MO plus 150 pg hSTING-mRNA. The phenotypes were analyzed at 72 hpf. (B) Survival rates of HSV-1-infected zebrafish rescued morphants. (C to E) Rescue effects were measured via real-time quantitative PCR (RT-PCR). Zebrafish embryos were injected with 3 ng STING morpholino plus 150 pg STING-mRNA from zebrafish, mouse, or human and then challenged with 200 PFU wild-type HSV-1 at 72 hpf. Induction of IFN-φ1 (C), ISG15 (D), and viperin (E) mRNAs was measured by real-time quantitative PCR at the indicated time points. (F to H) The STING loss-of function mutation cannot rescue deficient antiviral gene induction in STING morphants. Zebrafish embryos were injected with 3 ng control morpholino, 3 ng STING morpholino, or 3 ng STING morpholino plus 150 pg STING-mRNA from zebrafish full-length or loss-of-function mutation (S373A) STING. The larvae were infected with 200 PFU wild-type HSV-1 at 72 hpf. Expression levels of IFN-φ1 (F), ISG15 (G), and viperin (H) were measured by real-time quantitative PCR at the indicated time points. Assays were performed on RNA extracted from entire larvae and measured values normalized to the control set. Data shown are mean ± SEM from at least three independent experiments. *, $P < 0.05$; **, $P < 0.01$ (versus the corresponding control).

beled probe complementary to the HSV-1 ICP0 gene. HSV-1 began to appear as early as 24 hpi and increased steadily up to 48 hpi, which echoes the patterns of the antiviral gene expression induced by HSV-1. Notably, the HSV-1 focused predominantly in the brains and eyes of the larvae, and the virus was observed around the yolk sac (Fig. 3F, arrowheads).

To substantiate the localization of HSV-1 *in vivo*, we infected 72-hpf zebrafish larvae intravenously with HSV-1-GFP, an intact

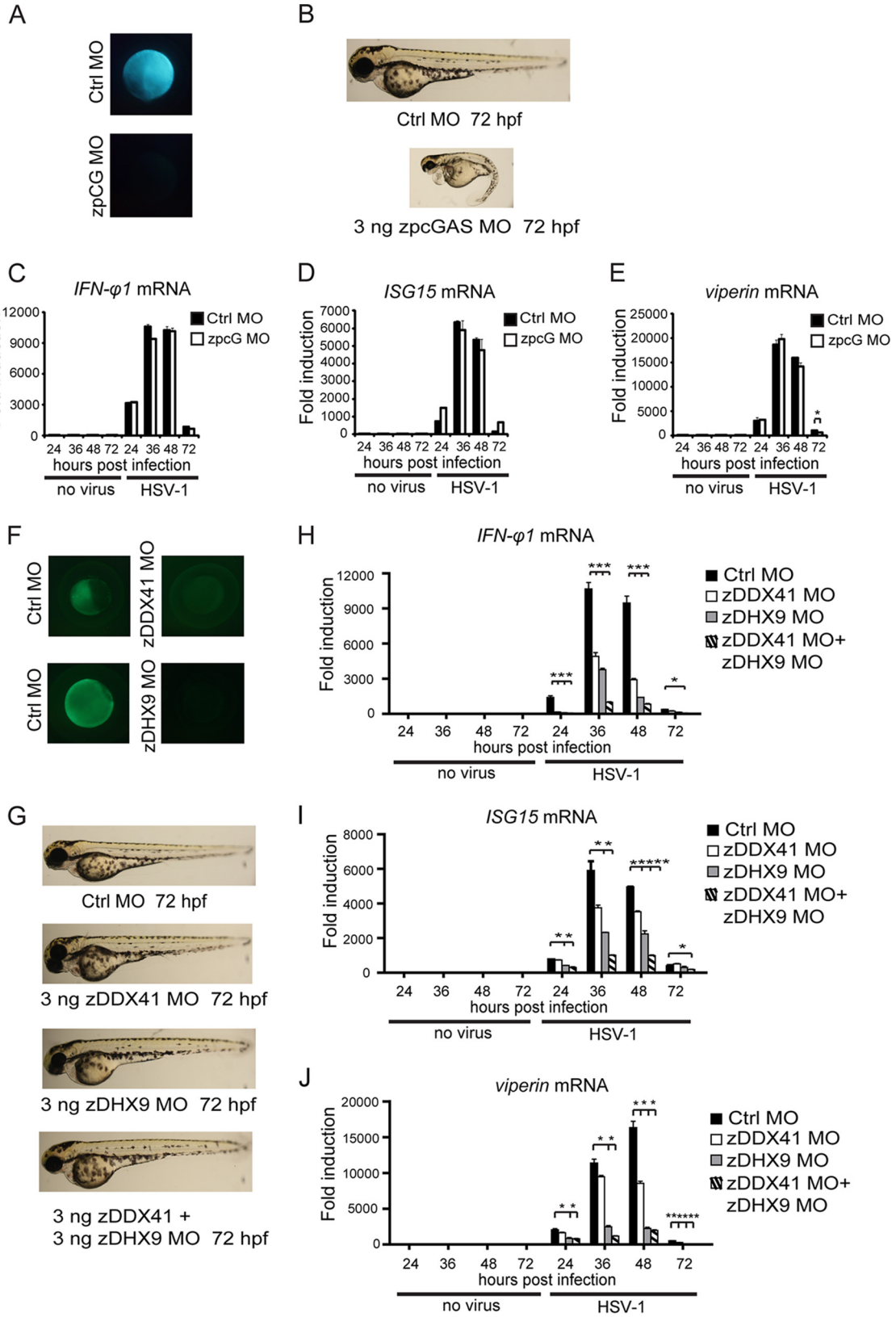

FIG 6 DDX41 and DHX9, but not cGAS, are indispensable for the innate immune response against HSV-1 infection. (A) Morpholino-based zpcGAS gene knockdown is efficient in zebrafish embryos. (B) Phenotypic analyses of zebrafish larvae at 72 hpf. Embryos were injected with 3 ng control morpholino (Ctrl.MO) or 3 ng zpcGAS MO and analyzed at 72 hpf. (C to E) Antiviral gene induction in HSV-1-infected control and cGAS morphant larvae. AB embryos were injected with 3 ng control morpholino or zebrafish predicted cGAS morpholino. The morphant larvae were stimulated with wild-type HSV-1 (200 PFU) for the

virus labeled with GFP. Consistently, the GFP pattern of the HSV-1 infection was identical to those with the WISH data, present in the entire body of the zebrafish larva and accumulated mostly in the brain, suggesting that the brain served as the reservoir for HSV-1 (Fig. 3G). Taken together, these data indicate that HSV-1 propagates successfully in brain and induces robust antiviral responses in zebrafish larvae.

Zebrafish STING is indispensable for sensing HSV-1 infection. Bioinformatics analysis revealed that STING is relatively conserved through vertebrate species (30). The zebrafish STING displayed 40.6% and 42% identity to human and mouse, respectively (data not shown). It is well established in the mouse model that the ER protein STING is indispensable for sensing and responding to HSV-1 infection (25). To explore the antiviral function of STING in zebrafish, we designed antisense morpholino oligonucleotides (MOs), which are effective for knocking down STING *in vivo* (zST MO). A scramble morpholino sequence (Gene Tool Ltd.) was included as negative control (Ctrl.MO) (Fig. 4A). The knockdown of the endogenous STING caused some minor developmental abnormities (shortened trunk and decreased pigmentation) (Fig. 4B). It was observed that 90% of the STING-silenced morphants died within 3 days, whereas 60% of the infected control morphants remained alive (Fig. 4C). As expected, HSV-1 infection induced the robust expression of IFN and IFN-responsive genes in control morphants. Notably, the knockdown of STING almost abolished the inductions of the same antiviral genes (IFN-φ1, ISG15, and viperin), when infecting zebrafish with HSV-1 (Fig. 4D to F). In addition, confocal microscopy revealed that HSV-1-GFP propagated much more strongly in the STING-silenced morphants than in the control morphants (Fig. 4G). There was nearly a 2-fold increase of GFP signal in the STING-silenced morphants (Fig. 4H).

Next, we generated morpholino-resistant STING mRNAs from zebrafish, mouse, and human. The phenotype and survival rate caused by STING deficiency could be partially rescued by morpholino-resistant STING mRNAs (Fig. 5A and B). Interestingly, the impaired expression of IFN-φ1, ISG15, and viperin in the STING-silenced larvae could be rescued by the injection of the zebrafish STING mRNA when infecting the larvae with HSV-1. Notably, the STING mRNAs from mouse and human could partially rescue these gene inductions (Fig. 5C to E). In human, STING S366 is essential for its function (39). We identified the corresponding conserved zebrafish STING S373 and generated the S373A loss-of-function mutant. Consistently, the mutant failed to rescue the impaired expression of IFN-φ1, ISG15, and viperin in the STING-silenced larvae (Fig. 5F to H). Taken together, these data indicate that zebrafish STING is indispensable for sensing DNA virus, confirming the conservation of STING function.

DHX9 and DDX41, but not cGAS, are cytosolic sensors of HSV-1 infection. Several cytosolic DNA sensors have recently been identified in mammals, including cyclic GMP-AMP synthase (cGAS), DDX41, and DHX9 (20, 22, 23). cGAS was characterized to be indispensable for sensing HSV-1 infection in mouse and human (40). We noticed that zebrafish contains an ortholog of cGAS (XM_680019.3), as predicted via bioinformatics analysis. Therefore, we named it zpcGAS (for zebrafish predicted cGAS). We designed the antisense morpholino oligonucleotides (zpcG MO) that specifically blocked the translation initiation in the zpcGAS sequence (Fig. 6A). Knocking down zpcGAS resulted in marked developmental abnormities of zebrafish larvae, as evidenced by a curly tail, hindbrain atrophy, and decreased pigmentation (Fig. 6B). Unexpectedly, the knockdown of zpcGAS did not cause an obvious effect on the induction of IFN-φ1, ISG15, and viperin in zebrafish larvae in response to HSV-1 infection (Fig. 6C to E).

We also determined the potential orthologs of DDX41 (NM_201045.1) and DHX9 (NM_001201444.1) in zebrafish, based on the sequence comparison and conserved domain architectures. Following the knockdown of DDX41 or DHX9 with the corresponding antisense morpholino oligonucleotides individually, we checked the efficiency of the morpholino knockdown (Fig. 6F). There were no obvious developmental abnormalities observed in the morphants. In addition, the DDX41/DHX9 double knockdown morphant apparently developed normally (Fig. 6G).

To test the function of DDX41 and DHX9, we checked the HSV-1-induced expression of the antiviral genes. Interestingly, silencing of DDX41 markedly decreased the induction of IFN-φ1, ISG15, and viperin. Silencing of DHX9 resulted in more reduction of the same antiviral genes. Furthermore, the induction of the antiviral genes (IFN-φ1, ISG15, and viperin) was almost abolished in the DDX41/DHX9 double knockdown morphant (Fig. 6H to J). Collectively, these data indicate that DDX41 and DHX9, but not cGAS, are *bona fide* sensors of HSV-1 infection in zebrafish.

MAVS is marginally involved in sensing HSV-1 infection. MAVS is an essential adaptor on mitochondria for the RIG-I signaling of mammals and zebrafish (29). We investigated whether MAVS played a role in sensing HSV-1 infection in zebrafish. Antisense morpholino oligonucleotides against MAVS (zMAVS MO) were effective in zebrafish embryos (Fig. 7A). It was observed that the knockdown of MAVS led to little effect on the developmental indexes of zebrafish larvae (Fig. 7B). The IFN-φ1 induction was only marginally reduced in MAVS knockdown morphants. However, the induction of ISG15 and viperin was apparently intact in MAVS knockdown morphants compared to wild-type and control morphants (Fig. 7C to E). Taken together, these data indicate that MAVS is marginally involving in sensing HSV-1 infection in zebrafish, which is consistent with the observations in mouse.

DISCUSSION

HSV-1 infects mammalian cells and displays its DNA in the cytosol. HSV-1 infection in mouse represents a good model to elucidate how hosts sense/recognize the cytosolic aberrant DNAs and initiate innate antiviral responses. Several DNA sensors have been characterized in

indicated time periods. Induction of IFN-φ1 (C), ISG15 (D), and viperin (E) mRNAs was measured by real-time quantitative PCR. (F) Morpholino-based zDDX41 and zDHX9 gene knockdown is efficient in zebrafish embryos. (G) Phenotypic analyses of morphant larvae at 72 hpf. Embryos were injected with 3 ng control morpholino (Ctrl MO), 3 ng zDDX41 MO, 3 ng zDHX9 MO, and 3 ng zDDX41 plus 3 ng zDHX9 MO. The phenotypes were analyzed at 72 hpf. (H to J) Quantification of antiviral gene induction in control, DDX41, DHX9, and double knockdown morphant larvae infected with HSV-1. AB embryos were injected with 3 ng control, DDX41, DHX9, or DDX41 and DHX9 morpholino. The morphant larvae were challenged with 200 PFU wild-type HSV-1 for the indicated time periods. Induction of IFN-φ1 (H), ISG15 (I), and viperin (J) mRNAs was measured by real-time quantitative PCR. Measured values were normalized to the mean of the control set. Data shown are mean ± SEM from at least three independent experiments. *, $P < 0.05$; **, $P < 0.01$ (versus the corresponding control).

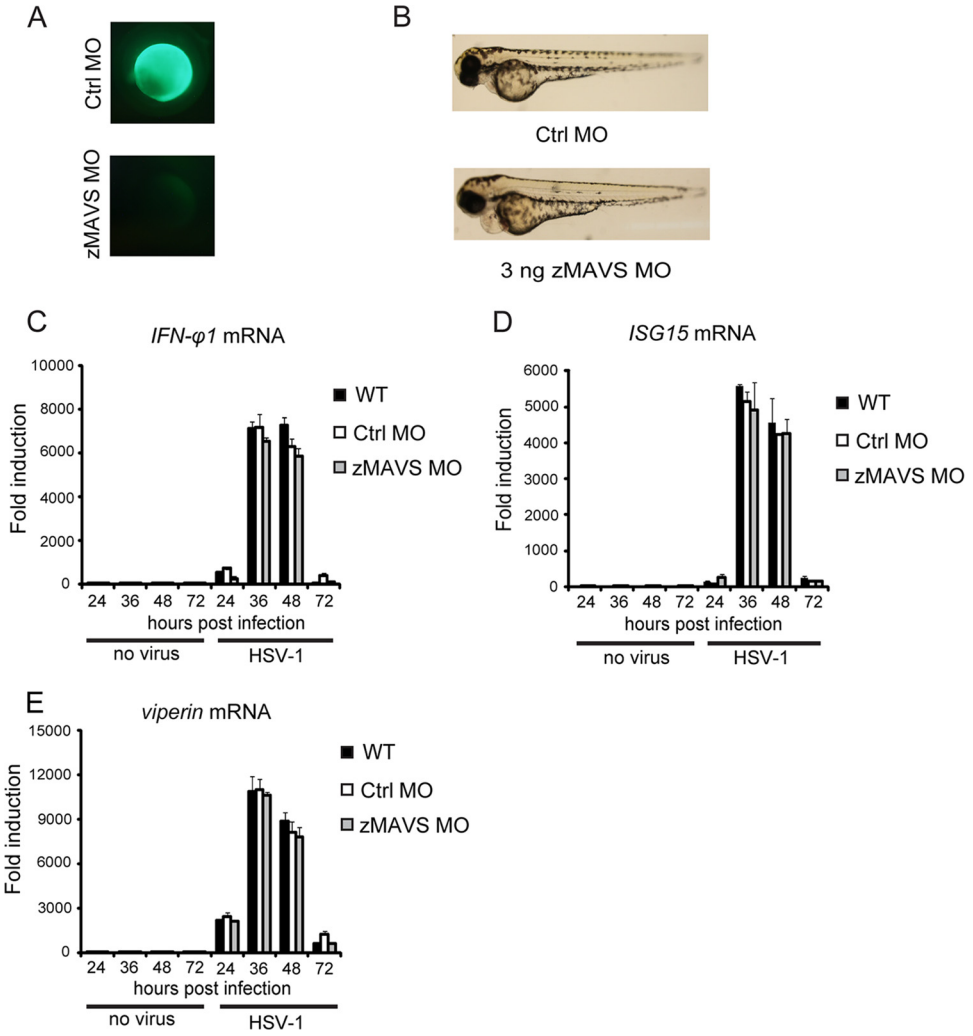

FIG 7 MAVS is marginally involved in the innate immune response against HSV-1 infection. (A) Morpholino-based zMAVS gene knockdown is efficient in zebrafish embryos. (B) Phenotypic analyses of zebrafish larvae at 72 hpf. Embryos were injected with 3 ng control morpholino (Ctrl.MO) or 3 ng zMAVS MO and analyzed at 72 hpf. (C to E) Antiviral gene induction in HSV-1infected control and MAVS morphants larvae. AB embryos were injected with 3 ng control morpholino or zebrafish MAVS morpholino. The morphant larvae were stimulated with 200 PFU wild-type HSV-1 for the indicated time periods. Induction of IFN-φ1 (C), ISG15 (D), and viperin (E) mRNAs was measured by real-time quantitative PCR. Data shown are mean ± SEM from at least three independent experiments. *, $P < 0.05$; **, $P < 0.01$ (versus the corresponding control).

mouse, including cGAS, DDX41, and DHX9. These receptors transmit the activation signal to the ER-resident protein STING, which in turn activates the TBK1 kinase and IRF3 transcriptional factor and ultimately induces the expression of a broad array of cytokines and chemokines which are important for innate immunity. Understanding of STING signaling is still in its infancy. More signaling and regulatory proteins are expected to be identified and characterized (37, 41–43). Given the versatility of zebrafish for genetic screening, we were interested in the feasibility of establishing an *in vivo* model to dissect the cytosolic DNA sensing pathway in zebrafish.

Mammal-tropic viruses are normally adapted to propagate at 37°C and fail to replicate at 28°C, a temperature optimal for zebrafish growth. This limits the successful establishment of most human disease-related virus infection models in zebrafish. In contrast, Chikungunya virus (CHIKV) triggers a strong type I interferon (IFN) response in zebrafish neutrophils and hepatocytes (11). Infectious hematopoietic necrosis virus (IHNV) primarily infects the vascular endothelium of zebrafish larvae (10). Infectious spleen and kidney necrosis virus (ISKNV) could replicate in almost all organs of the infected adult zebrafish (12). Unfortunately, few studies of these viruses have been systematically performed in mice, which restrict their application in elucidating the relevant innate immune signaling.

A recent study demonstrates that adult zebrafish are susceptible to HSV-1 infection and that HSV-1 colonizes the zebrafish encephalon and spinal cord (13). In this study, we confirm that HSV-1 could infect zebrafish successfully at 28°C. Notably, the HSV-1 infection pattern in zebrafish nicely mirrors that in mouse, in terms of the infection time course, the location of colonization, and the establishment of lytic/latency phases (25). Importantly, we have optimized the time windows of the HSV-1 infection at the different developmental stages of zebrafish larvae, and we found 72 hpf to be the best stage for administering HSV-1 infection. As a result, we have reduced the dose of HSV-1 from the former 10^4 to 10^6 PFU to approximately 200 PFU, which makes future screening experiments possible.

As a pilot test, we systematically checked the induction of antiviral genes in zebrafish during HSV-1 infection. We observed that HSV-1 robustly induced the expression of the IFN-φ1, ISG15, and viperin genes in zebrafish, indicating that zebrafish is fully competent to sense HSV-1 and initiate innate antiviral responses. The RIG-I/MAVS signaling is conserved in zebrafish, and it responds specifically to RNA virus infection (29, 30). Consistently, silencing of zebrafish MAVS did not affect the innate antiviral responses to the HSV-1 infection, which substantiates the observation in mouse (44).

Notably, silencing of zebrafish STING almost completely abolished the induction of IFN-φ1, ISG15, and viperin by HSV-1. This effect could be rescued by reintroducing the morpholino-resistant mRNA of zebrafish STING. It could also be partially rescued by reintroducing the morpholino-resistant mRNAs of human or mouse STING. Notably, the conserved loss-of-function mutant of STING (S373A) failed to display the rescuing effects. These data indicate that zebrafish STING performs the same function as its orthologs in mammals. The HSV-1 infection model in zebrafish apparently reproduces that in mouse.

Unexpectedly, the predicted zebrafish cGAS was dispensable for sensing HSV-1 in zebrafish. One possibility is that the bioinformatics algorithm breaks down in this case, because the zebrafish cGAS ortholog does not necessarily have detectable sequential identity to its mammalian counterparts. Another possibility is that zebrafish does not have the cGAS functional counterpart at all. cGAS is not present in all mouse cell types, and its antiviral function is replaced by other DNA sensors in specific cell types (45). We speculate that cGAS probably evolved later in the animal domain. This speculation is partly supported by the observation that silencing of DDX41 and DHX9 markedly impaired the expression of the HSV-1-triggered antiviral genes in zebrafish. Future evolutionary analysis might underscore the functional redundancy and/or diversification of these DNA sensors across species.

A STING knockout mouse is viable (25), and so is the STING-silenced zebrafish. A DDX41 or DHX9 knockout mouse is currently unavailable. The DDX41- or DHX9-silenced zebrafish is developmentally normal. Therefore, we speculated that STING, DDX41, and DHX9 mediated mainly the innate immunity in zebrafish, which makes it easier to dissect the cytosolic DNA sensing pathway in zebrafish. Collectively, our current study has successfully established an HSV-1 infection model in zebrafish that reproduces the antiviral responses observed in the mouse model. This model will be instrumental for discovering the key signaling proteins in STING signaling and uncovering the conservation and diversification of the DNA sensing pathways. The HSV-1 infection model is also useful for screening agonists or antagonists of the STING signaling pathway, which are potentially important for manipulating inflammation and autoimmune diseases.

ACKNOWLEDGMENTS

Chen Wang was supported by grants from the National Natural Science Foundation of China (31030021 and 81161120542) and the Ministry of Science and Technology of China (2012CB910200 and 2011CB910904).

We have no financial conflicts of interest.

REFERENCES

1. **Kimmel CB, Ballard WW, Kimmel SR, Ullmann B, Schilling TF.** 1995. Stages of embryonic development of the zebrafish. Dev Dyn **203:**253–310. http://dx.doi.org/10.1002/aja.1002030302.
2. **Trede NS, Langenau DM, Traver D, Look AT, Zon LI.** 2004. The use of zebrafish to understand immunity. Immunity **20:**367–379. http://dx.doi.org/10.1016/S1074-7613(04)00084-6.
3. **Traver D, Herbomel P, Patton EE, Murphey RD, Yoder JA, Litman GW, Catic A, Amemiya CT, Zon LI, Trede NS.** 2003. The zebrafish as a model organism to study development of the immune system. Adv Immunol **81:**253–330.
4. **Kanther M, Rawls JF.** 2010. Host-microbe interactions in the developing zebrafish. Curr Opin Immunol **22:**10–19. http://dx.doi.org/10.1016/j.coi.2010.01.006.
5. **Amsterdam A, Nissen RM, Sun Z, Swindell EC, Farrington S, Hopkins N.** 2004. Identification of 315 genes essential for early zebrafish development. Proc Natl Acad Sci U S A **101:**12792–12797. http://dx.doi.org/10.1073/pnas.0403929101.
6. **Lieschke GJ, Currie PD.** 2007. Animal models of human disease: zebrafish swim into view. Nat Rev Genet **8:**353–367. http://dx.doi.org/10.1038/nrg2091.
7. **Ramakrishnan L.** 2012. Revisiting the role of the granuloma in tuberculosis. Nat Rev Immunol **12:**352–366. http://dx.doi.org/10.1038/nri3211.
8. **Langenau DM, Ferrando AA, Traver D, Kutok JL, Hezel JP, Kanki JP, Zon LI, Look AT, Trede NS.** 2004. In vivo tracking of T cell development, ablation, and engraftment in transgenic zebrafish. Proc Natl Acad Sci U S A **101:**7369–7374. http://dx.doi.org/10.1073/pnas.0402248101.
9. **Bernier R, Golzio C, Xiong B, Stessman HA, Coe BP, Penn O, Witherspoon K, Gerdts J, Baker C, Vulto-van Silfhout AT, Schuurs-Hoeijmakers JH, Fichera M, Bosco P, Buono S, Alberti A, Failla P, Peeters H, Steyaert J, Vissers LE, Francescatto L, Mefford HC, Rosenfeld JA, Bakken T, O'Roak BJ, Pawlus M, Moon R, Shendure J, Amaral DG, Lein E, Rankin J, Romano C, de Vries BB, Katsanis N, Eichler EE.** 2014. Disruptive CHD8 mutations define a subtype of autism early in development. Cell **158:**263–276. http://dx.doi.org/10.1016/j.cell.2014.06.017.
10. **Ludwig M, Palha N, Torhy C, Briolat V, Colucci-Guyon E, Bremont M, Herbomel P, Boudinot P, Levraud JP.** 2011. Whole-body analysis of a viral infection: vascular endothelium is a primary target of infectious hematopoietic necrosis virus in zebrafish larvae. PLoS Pathog **7:**e1001269. http://dx.doi.org/10.1371/journal.ppat.1001269.
11. **Palha N, Guivel-Benhassine F, Briolat V, Lutfalla G, Sourisseau M, Ellett F, Wang CH, Lieschke GJ, Herbomel P, Schwartz O, Levraud JP.** 2013. Real-time whole-body visualization of Chikungunya virus infection and host interferon response in zebrafish. PLoS Pathog **9:**e1003619. http://dx.doi.org/10.1371/journal.ppat.1003619.
12. **Xu X, Zhang L, Weng S, Huang Z, Lu J, Lan D, Zhong X, Yu X, Xu A, He J.** 2008. A zebrafish (Danio rerio) model of infectious spleen and kidney necrosis virus (ISKNV) infection. Virology **376:**1–12. http://dx.doi.org/10.1016/j.virol.2007.12.026.
13. **Burgos JS, Ripoll-Gomez J, Alfaro JM, Sastre I, Valdivieso F.** 2008. Zebrafish as a new model for herpes simplex virus type 1 infection. Zebrafish **5:**323–333. http://dx.doi.org/10.1089/zeb.2008.0552.
14. **Sanders GE, Batts WN, Winton JR.** 2003. Susceptibility of zebrafish (Danio rerio) to a model pathogen, spring viremia of carp virus. Comp Med **53:**514–521.
15. **Novoa B, Romero A, Mulero V, Rodriguez I, Fernandez I, Figueras A.** 2006. Zebrafish (Danio rerio) as a model for the study of vaccination against viral haemorrhagic septicemia virus (VHSV). Vaccine **24:**5806–5816. http://dx.doi.org/10.1016/j.vaccine.2006.05.015.
16. **Nakhaei P, Genin P, Civas A, Hiscott J.** 2009. RIG-I-like receptors: sensing and responding to RNA virus infection. Semin Immunol **21:**215–222. http://dx.doi.org/10.1016/j.smim.2009.05.001.
17. **Paludan SR, Bowie AG.** 2013. Immune sensing of DNA. Immunity **38:**870–880. http://dx.doi.org/10.1016/j.immuni.2013.05.004.
18. **Seth RB, Sun L, Ea CK, Chen ZJ.** 2005. Identification and characterization of MAVS, a mitochondrial antiviral signaling protein that activates NF-kappaB and IRF 3. Cell **122:**669–682. http://dx.doi.org/10.1016/j.cell.2005.08.012.
19. **Honda K, Takaoka A, Taniguchi T.** 2006. Type I interferon [corrected] gene induction by the interferon regulatory factor family of transcription

factors. Immunity **25:**349–360. http://dx.doi.org/10.1016/j.immuni.2006.08.009.
20. **Sun L, Wu J, Du F, Chen X, Chen ZJ.** 2013. Cyclic GMP-AMP synthase is a cytosolic DNA sensor that activates the type I interferon pathway. Science **339:**786–791. http://dx.doi.org/10.1126/science.1232458.
21. **Unterholzner L, Keating SE, Baran M, Horan KA, Jensen SB, Sharma S, Sirois CM, Jin T, Latz E, Xiao TS, Fitzgerald KA, Paludan SR, Bowie AG.** 2010. IFI16 is an innate immune sensor for intracellular DNA. Nat Immunol **11:**997–1004. http://dx.doi.org/10.1038/ni.1932.
22. **Zhang Z, Yuan B, Lu N, Facchinetti V, Liu YJ.** 2011. DHX9 pairs with IPS-1 to sense double-stranded RNA in myeloid dendritic cells. J Immunol **187:**4501–4508. http://dx.doi.org/10.4049/jimmunol.1101307.
23. **Parvatiyar K, Zhang Z, Teles RM, Ouyang S, Jiang Y, Iyer SS, Zaver SA, Schenk M, Zeng S, Zhong W, Liu ZJ, Modlin RL, Liu YJ, Cheng G.** 2012. The helicase DDX41 recognizes the bacterial secondary messengers cyclic di-GMP and cyclic di-AMP to activate a type I interferon immune response. Nat Immunol **13:**1155–1161. http://dx.doi.org/10.1038/ni.2460.
24. **Broz P, Monack DM.** 2013. Newly described pattern recognition receptors team up against intracellular pathogens. Nat Rev Immunol **13:**551–565. http://dx.doi.org/10.1038/nri3479.
25. **Ishikawa H, Ma Z, Barber GN.** 2009. STING regulates intracellular DNA-mediated, type I interferon-dependent innate immunity. Nature **461:**788–792. http://dx.doi.org/10.1038/nature08476.
26. **Sun W, Li Y, Chen L, Chen H, You F, Zhou X, Zhou Y, Zhai Z, Chen D, Jiang Z.** 2009. ERIS, an endoplasmic reticulum IFN stimulator, activates innate immune signaling through dimerization. Proc Natl Acad Sci U S A **106:**8653–8658. http://dx.doi.org/10.1073/pnas.0900850106.
27. **Zhong B, Yang Y, Li S, Wang YY, Li Y, Diao F, Lei C, He X, Zhang L, Tien P, Shu HB.** 2008. The adaptor protein MITA links virus-sensing receptors to IRF3 transcription factor activation. Immunity **29:**538–550. http://dx.doi.org/10.1016/j.immuni.2008.09.003.
28. **Jin L, Waterman PM, Jonscher KR, Short CM, Reisdorph NA, Cambier JC.** 2008. MPYS, a novel membrane tetraspanner, is associated with major histocompatibility complex class II and mediates transduction of apoptotic signals. Mol Cell Biol **28:**5014–5026. http://dx.doi.org/10.1128/MCB.00640-08.
29. **Biacchesi S, LeBerre M, Lamoureux A, Louise Y, Lauret E, Boudinot P, Bremont M.** 2009. Mitochondrial antiviral signaling protein plays a major role in induction of the fish innate immune response against RNA and DNA viruses. J Virol **83:**7815–7827. http://dx.doi.org/10.1128/JVI.00404-09.
30. **Biacchesi S, Merour E, Lamoureux A, Bernard J, Bremont M.** 2012. Both STING and MAVS fish orthologs contribute to the induction of interferon mediated by RIG-I. PLoS One **7:**e47737. http://dx.doi.org/10.1371/journal.pone.0047737.
31. **Sun F, Zhang YB, Liu TK, Shi J, Wang B, Gui JF.** 2011. Fish MITA serves as a mediator for distinct fish IFN gene activation dependent on IRF3 or IRF7. J Immunol **187:**2531–2539. http://dx.doi.org/10.4049/jimmunol.1100642.
32. **Aggad D, Mazel M, Boudinot P, Mogensen KE, Hamming OJ, Hartmann R, Kotenko S, Herbomel P, Lutfalla G, Levraud JP.** 2009. The two groups of zebrafish virus-induced interferons signal via distinct receptors with specific and shared chains. J Immunol **183:**3924–3931. http://dx.doi.org/10.4049/jimmunol.0901495.
33. **Levraud JP, Boudinot P, Colin I, Benmansour A, Peyrieras N, Herbomel P, Lutfalla G.** 2007. Identification of the zebrafish IFN receptor: implications for the origin of the vertebrate IFN system. J Immunol **178:**4385–4394. http://dx.doi.org/10.4049/jimmunol.178.7.4385.
34. **Langevin C, Aleksejeva E, Passoni G, Palha N, Levraud JP, Boudinot P.** 2013. The antiviral innate immune response in fish: evolution and conservation of the IFN system. J Mol Biol **425:**4904–4920. http://dx.doi.org/10.1016/j.jmb.2013.09.033.
35. **Langevin C, van der Aa LM, Houel A, Torhy C, Briolat V, Lunazzi A, Harmache A, Bremont M, Levraud JP, Boudinot P.** 2013. Zebrafish ISG15 exerts a strong antiviral activity against RNA and DNA viruses and regulates the interferon response. J Virol **87:**10025–10036. http://dx.doi.org/10.1128/JVI.01294-12.
36. **Paludan SR, Bowie AG, Horan KA, Fitzgerald KA.** 2011. Recognition of herpesviruses by the innate immune system. Nat Rev Immunol **11:**143–154. http://dx.doi.org/10.1038/nri2937.
37. **Wang Q, Liu X, Cui Y, Tang Y, Chen W, Li S, Yu H, Pan Y, Wang C.** 2014. The E3 ubiquitin ligase AMFR and INSIG1 bridge the activation of TBK1 kinase by modifying the adaptor STING. Immunity **41:**919–933. http://dx.doi.org/10.1016/j.immuni.2014.11.011.
38. **Antoine TE, Jones KS, Dale RM, Shukla D, Tiwari V.** 2014. Zebrafish: modeling for herpes simplex virus infections. Zebrafish **11:**17–25. http://dx.doi.org/10.1089/zeb.2013.0920.
39. **Tanaka Y, Chen ZJ.** 2012. STING specifies IRF3 phosphorylation by TBK1 in the cytosolic DNA signaling pathway. Sci Signal **5:**ra20. http://dx.doi.org/10.1126/scisignal.2002521.
40. **Ablasser A, Goldeck M, Cavlar T, Deimling T, Witte G, Rohl I, Hopfner KP, Ludwig J, Hornung V.** 2013. cGAS produces a 2′-5′-linked cyclic dinucleotide second messenger that activates STING. Nature **498:**380–384. http://dx.doi.org/10.1038/nature12306.
41. **Zhou Q, Lin H, Wang S, Wang S, Ran Y, Liu Y, Ye W, Xiong X, Zhong B, Shu HB, Wang YY.** 2014. The ER-associated protein ZDHHC1 is a positive regulator of DNA virus-triggered, MITA/STING-dependent innate immune signaling. Cell Host Microbe **16:**450–461. http://dx.doi.org/10.1016/j.chom.2014.09.006.
42. **Zhang L, Mo J, Swanson KV, Wen H, Petrucelli A, Gregory SM, Zhang Z, Schneider M, Jiang Y, Fitzgerald KA, Ouyang S, Liu ZJ, Damania B, Shu HB, Duncan JA, Ting JP.** 2014. NLRC3, a member of the NLR family of proteins, is a negative regulator of innate immune signaling induced by the DNA sensor STING. Immunity **40:**329–341. http://dx.doi.org/10.1016/j.immuni.2014.01.010.
43. **Cai X, Chiu YH, Chen ZJ.** 2014. The cGAS-cGAMP-STING pathway of cytosolic DNA sensing and signaling. Mol Cell **54:**289–296. http://dx.doi.org/10.1016/j.molcel.2014.03.040.
44. **Cotter CR, Kim WK, Nguyen ML, Yount JS, Lopez CB, Blaho JA, Moran TM.** 2011. The virion host shutoff protein of herpes simplex virus 1 blocks the replication-independent activation of NF-kappaB in dendritic cells in the absence of type I interferon signaling. J Virol **85:**12662–12672. http://dx.doi.org/10.1128/JVI.05557-11.
45. **Wu X, Wu FH, Wang X, Wang L, Siedow JN, Zhang W, Pei ZM.** 2014. Molecular evolutionary and structural analysis of the cytosolic DNA sensor cGAS and STING. Nucleic Acids Res **42:**8243–8257. http://dx.doi.org/10.1093/nar/gku569.